Fuel 178 (2016) 234–242

Contents lists available at ScienceDirect

Fuel

journal homepage: www.elsevier.com/locate/fuel

Electrokinetic behavior of asphaltene particles

Ali Hosseini [a], Elnaz Zare [b], Shahab Ayatollahi [a], Francisco M. Vargas [c], Walter G. Chapman [c], Konstantinos Kostarelos [d,*], Vahid Taghikhani [a,c]

[a] Department of Chemical and Petroleum Engineering, Sharif University of Technology, Tehran, Iran
[b] School of Chemical and Petroleum Engineering, Shiraz University, Shiraz, Iran
[c] Department of Chemical and Biomolecular Engineering, Rice University, Houston, TX, USA
[d] Petroleum Engineering Program, The University of Houston, Houston, TX, USA

ARTICLE INFO

Article history:
Received 12 November 2015
Received in revised form 22 January 2016
Accepted 14 March 2016
Available online 21 March 2016

Keywords:
Asphaltene
Electrostatic field
Asphaltene aggregation
Electro-deposition
Asphaltene electro-kinetics

ABSTRACT

The effect of electrostatic field on the aggregation rate and aggregate size of asphaltene particles precipitated from three different crude oil samples suspended in a mixture of toluene and n-heptane (a model oil) was investigated. An electrode-embedded glass micro-model utilizing a high-voltage direct current power supply was utilized in this study. The asphaltene particle size and the rate of aggregation under the electric field were monitored using a high-resolution optical microscope and the average aggregate size for asphaltene particles was estimated using image processing software. To investigate the effects of structural parameters on asphaltene aggregation rate, aggregate size and electro-deposition, the elemental analyses for the three asphaltene samples were carried out and the mass ratios for C, H, N, S and O elements present in the asphaltene samples were determined. Also, the functional groups of asphaltene molecules were analyzed using the FTIR technique. Asphaltene molecules with larger chromophore and higher complexity exhibited faster aggregation behavior under the electrical field. The asphaltene aggregation rate was found to be directly proportional to the number of hetero-atoms on asphaltene molecules. The effects of parameters such as the electric field intensity, exposure time, asphaltene concentration, the amount of precipitant, and the asphaltene molecular structure on the asphaltene aggregation rate and aggregate size under the electrostatic field were also investigated. The electrostatic field strongly affected the aggregation rate of asphaltene particle; under an electrostatic field, asphaltene particles tended to aggregate faster and this may have resulted in faster and a larger quantity of asphaltene particles that precipitated out of the quiescent mixture of toluene and n-heptane. It should be also stated that for higher voltage applied to the mixture, a higher aggregation rate and larger aggregate size of asphaltene particles were observed.

1. Introduction

Asphaltene is a heavy fraction of crude oil with a complex poly-aromatic structure that is soluble in aromatic solvents such as toluene but insoluble in light normal alkanes such as n-pentane and n-heptane [1–4]. Interest in the characteristics and properties of asphaltene originates from the severe operational problems caused at the different stages of petroleum production due to asphaltene phase separation, asphaltene flocculation and deposition [5]. Identifying the conditions leading to asphaltene precipitation from crude oils has been a major challenge for researchers over the past decades, and many attempts have been made to understand the effects of several parameters such as pressure, temperature and crude composition on asphaltene phase behavior [1,6–10]. It has been recently shown that, due to the molecular complexity and high polarity of the asphaltene molecules, their electro-kinetic behavior such as natural streaming potential can have an important role in their instability and, hence, in their precipitation and deposition tendencies [11–17]. The electro-kinetic properties such as electrical conductivity, electrophoresis and electro-deposition of asphaltene particles under an electrostatic field have been extensively studied [11,12,16,18,19]. In these publications, it has been shown that asphaltene molecules can be polarized and gain electric charge while they are exposed to the electrostatic field. It should be emphasized that neither the mechanism of asphaltene charging nor the conditions leading to electro-deposition have been well

* Corresponding author.

http://dx.doi.org/10.1016/j.fuel.2016.03.051
0016-2361/

understood to date. In most studies, it has been concluded that asphaltene molecules possess a predominantly positive charge in a number of non-aqueous solvents such as nitromethane [20], heptane [21], ethanol [21], and mixtures of heptane and toluene [22]. On the other hand, negatively-charged asphaltene deposits were observed in experiments conducted in crude oil samples [14,19,23,24]. An electrostatic field can be utilized for various applications in the petroleum production and processing such as the electric de-emulsification [25] in which direct current electric voltage is applied to break water–oil emulsions [14]. It should be mentioned that the precipitation of asphaltene molecules has been previously described based on the electrical charge interactions between asphaltene and resin molecules in crude oil. It is controversially believed that the resin content has the greatest impact on the stability of asphaltene molecules in crude oil and that the resin-asphaltene molecular interaction is highly dominated by the opposing surface charges of resins and asphaltene moieties [13]. Any disruptions in such electrostatic and surface charge interactions between asphaltene and resins can change the attraction forces and result in the destabilization of colloidal asphaltene particles [26,27]. Recent studies on the electrical conductivity of asphaltene particles have broadened the understanding of their molecular association [28,29], however, studies on solid asphaltene electrical conductivity showed that solid asphaltene particles mimic semiconductor behavior. It has been observed that due to the structural phase transition, the conductivity increases at higher temperatures [30]. More detailed investigations of asphaltene electro-kinetics such as electrophoresis, and adsorption properties using different crude oils strongly confirmed the charge-bearing characteristics and streaming potential of asphaltene molecules [22,31–33]. It was concluded that protonation and dissociation reactions of asphaltene functional groups results in asphaltene surface charging and its electrophoretic mobility [34]. However, solvent-induced polarity causes reversed electrophoretic mobility of destabilized asphaltene particles. Asphaltene particles dispersed in a polar solvent (water) present a negative electrophoretic mobility, whereas when dispersed in a non-polar solvent (toluene), the particles present positive electrophoretic mobility [33]. In this way it has been shown that the net negative surface charge of colloidal asphaltene is the main cause of deposition on metal pipes due to potential differences across them [7]. Such charge neutralization might be used to manage and control the asphaltene precipitation and deposition [35]. A recent study by Hashmi and Firoozabadi [36] tried to elucidate the existing vagueness of asphaltene surface charge; they suggested that asphaltene particles possess heterogeneous surface charges where some moieties may exhibit a small net positive charge and others a negative surface charge. Other parameters such as metallic components and acid–base functional groups contribute to the surface charge, which may vary with the source of the crude oil, and other characteristics of the crude oils such the molecular weights and densities [36].

In this work, asphaltene particles were precipitated from three different crude oil samples and added to a mixture of toluene and n-heptane in order to understand their electro-kinetic behavior. A glass micro model was equipped with two electrodes, an optical microscope, and a high-voltage, direct current (HVDC) power supply. To understand the effects of structural parameters on asphaltene aggregation rate and aggregate size, elemental analyses of the three asphaltene samples were conducted and the mass ratios of C, H, N, S and O elements were determined. Also, the effects of parameters such as electric field intensity, exposure time, asphaltene concentration, and precipitant strength on the asphaltene aggregation and electro-deposition were investigated.

2. Materials and methods

Asphaltene particles were precipitated from three crude oil samples having three different API gravity using the standard ASTM-D6560-12 method [37]. The results of SARA (saturates, aromatics, resin, and asphaltene) analyses for these three crude oil samples are presented in Table 1. As shown in Table 1, the heaviest crude oil with API = 12.8 is labeled as "Type A", the crude oil with medium API gravity (23.8) is labeled as "Type B" and the lightest crude oil (API = 31) is labeled as "Type C". This nomenclature will be used throughout this manuscript for the crude oils and their corresponding asphaltene samples. The standard procedure of Clay-Gel Absorption Chromatographic method (ASTM D2007-93) was used for the SARA fractionation analysis.

To synthesize the model oil, normal heptane with a purity of 99.9% was purchased from Merck Company and used to precipitate the asphaltene particles from the above three crude oil samples. Toluene with the purity of 99% (Merck Co.) was used to dissolve the asphaltene particles. In order to prepare homogenous mixtures, the asphaltene particles were initially dissolved in toluene and stirred for one hour using a magnetic stirrer. Then, n-heptane was gradually added to the mixture and stirred for an additional 30 min. All samples were prepared at a heptane to toluene ratio of 30:70 except preliminary experiments aimed at studying the effect of precipitant (n-heptane) concentration. Prior to each experiment, the model oil was sonicated at a frequency of 40 kHz for two minutes to disperse all asphaltene particles uniformly and break any pre-formed aggregates or particles' cross-links. Moreover, to ensure that no asphaltene precipitation occurred during the preparation procedure, the concentration of asphaltene in the mixture or model oil was monitored using spectrophotometry [38]. It should be noted that the synthesis of this asphaltene suspension was performed at ambient temperature and at only two asphaltene concentrations, 1 g/l and 3 g/l. All of the electrokinetic tests were conducted under static conditions. For the sake of considering the precipitant effect on asphaltene aggregation, a set of preliminary experiments was conducted to observe whether the particles precipitated due to precipitant addition or the applied electrostatic field. These preliminary control experiments were performed at varying heptane concentrations in order to determine the visual on-set point of the asphaltene particles without applying the electrostatic field. It is a well-accepted in the literature that, in visual studies, the asphaltene on-set point is the point at which the average asphaltene particle size grows larger than 0.5 μm in diameter [39]. For most of the test solutions, it took at least 18 h for asphaltene particles to appear (to grow larger than 0.5 μm), whereas the duration for the electrostatic tests was less than two hours. We also note that, when applying an electrostatic force, the asphaltene particle grow about two orders of magnitude (greater than 10 μm) during the first minutes of the experiments alone.

3. Analysis of asphaltene chemical structure

Detailed analysis of three asphaltene samples in order to determine their chemical structures was done by Amin et al. [40] at the

Table 1
SARA analysis and the API gravity of crude oil used in this work.

	Crude Type A	Crude Type B	Crude Type C
Saturates (wt.%)	21.83	42.0	51.75
Aromatics (wt.%)	53.59	43.0	34.45
Resins (wt.%)	9.58	8.0	8.5
C7-Asphaltenes (wt.%)	14.7	7.0	5.3
API gravity (°)	12.8	23.8	31.0

Table 2
Elemental analysis of asphaltene samples.

Asphaltene	C (wt.%)	H (wt.%)	N (wt.%)	S (wt.%)	O (wt.%)	Ni (ppm)	V (ppm)	Formula
Type A	80.34	7.19	0.98	8.90	2.57	0.277	0.189	$C_{95}H_{102}O_2N_1S_4$
Type B	74.56	6.74	0.85	6.84	10.99	0.626	0.219	$C_{102}H_{110}O_{11}N_1S_3$
Type C	79.84	7.71	1.50	6.09	4.84	0.166	1.052	$C_{62}H_{71}O_3N_1S_2$

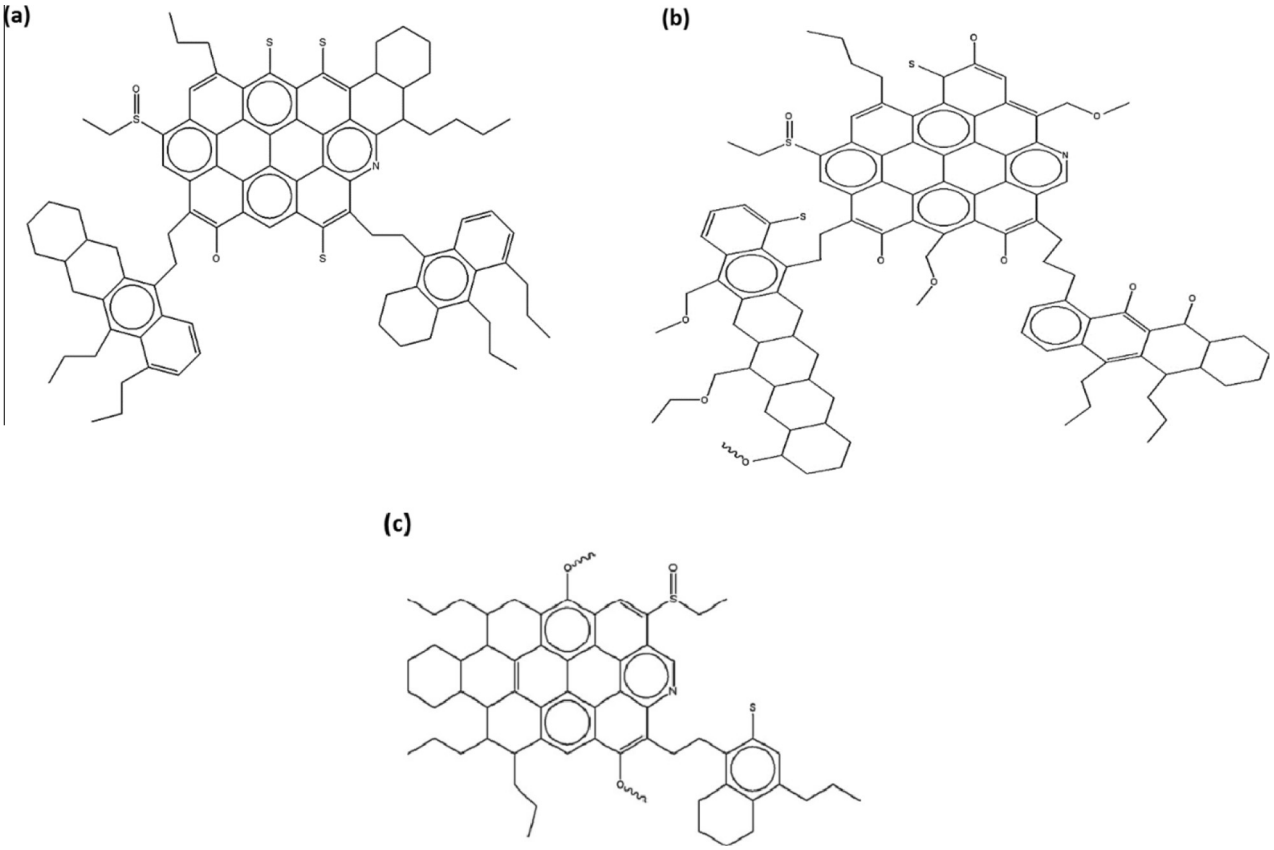

Fig. 1. Proposed molecular structure for: (a) asphaltene Type A; (b) asphaltene Type B; and (c) asphaltene Type C [40].

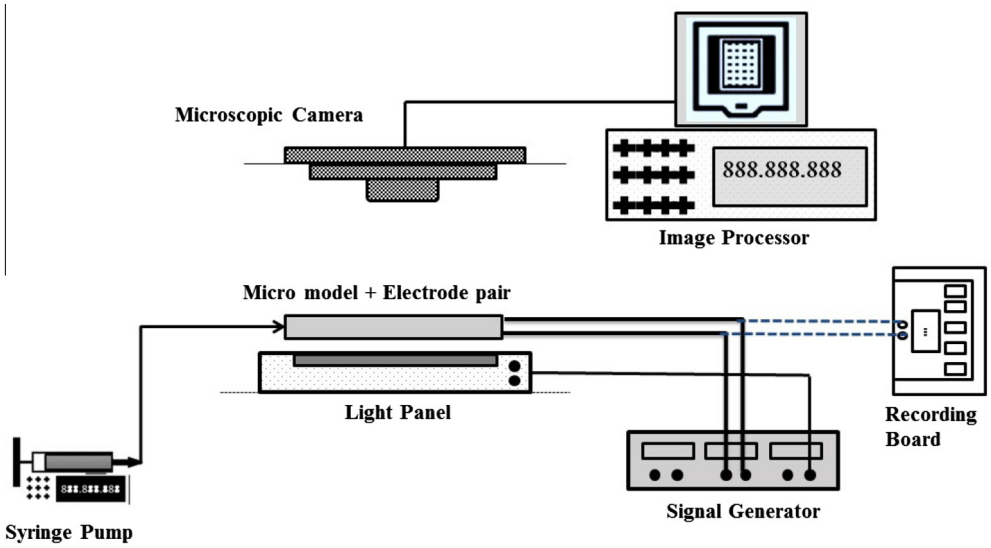

Fig. 2. Schematic diagram of the experimental set-up used in this study.

same research center using coupled elemental analysis, FTIR, and molecular simulations; the structural analysis was performed according to the procedures described elsewhere [40–42] and the results are reported in Table 2. The mass ratios of the C, H, N, S, and O elements present in the asphaltene molecules were determined using the elemental technique. The CHNSO analyzer (Thermo Flash EA 1112 series) was used for the elemental analysis. In addition, the amount of nickel (Ni) and vanadium (V) were given in Table 2. The molecular structure of each asphaltene sample was proposed based on the elemental mass ratios for each asphaltene sample. The presence of particular functional groups in each asphaltene sample was determined using the FTIR spectra (Shimadzu model 8300). Two peaks at 1325 and 1037 cm^{-1} are assigned to C–N and S–O groups stretching vibrations, respectively, while other peaks positioned at 3070 cm^{-1}, 2920 cm^{-1}, and 2850 cm^{-1} are indications of the aromatic and aliphatic hydrocarbons presence [40].

It is worth mentioning that deuterated chloroform (CD_3Cl) was used to determine both Proton NMR (H NMR) and Carbon NMR (C NMR) spectra. Both spectra were used to determine the ratios of carbon and hydrogen atoms contributing to aromatic and aliphatic parts of asphaltene molecules. This measurement leads to the estimation of the number of peripheral aliphatic chains and aromatic rings from which the chemical formula of each sample can be predicted.

The results of the elemental analysis, along with the FTIR spectra confirmed the existence of a large chromophore composed of at least seven fused rings and a small chromophore with two rings on each structure. The Type C asphaltene contains saturated hydrocarbon chains attached to the main large chromophore. These chains are composed of three carbon atoms and the main chromophore contains aromatic fused rings couple with non-aromatic rings. Asphaltene Type B has the largest chromophore consisting of eleven fused rings. Both Type A and B asphaltenes show evidence of aliphatic hydrocarbon chains with three carbon atoms. These structural features are very likely to control the mechanism of asphaltene precipitation and aggregation. Fig. 1 presents the proposed molecular structures of asphaltene Types A, B, and C based on molecular simulations performed using both elemental and FTIR data [40].

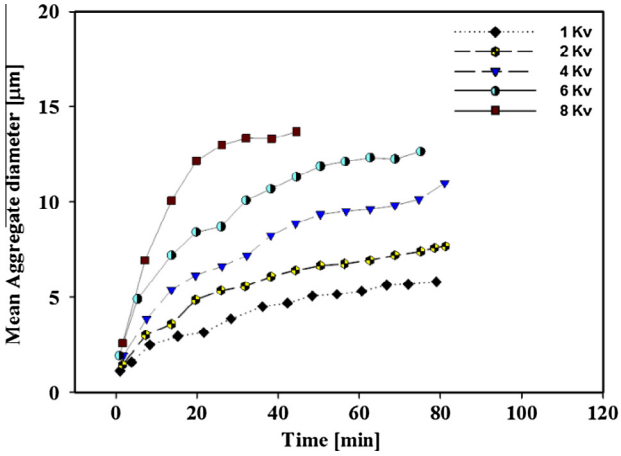

Fig. 4. Mean aggregate diameter in a model oil (1 g/l solution of asphaltene Type A) subjected to an electrostatic field for an 80-min duration. The measurements were repeated using voltages that varied between 1 and 8 kV.

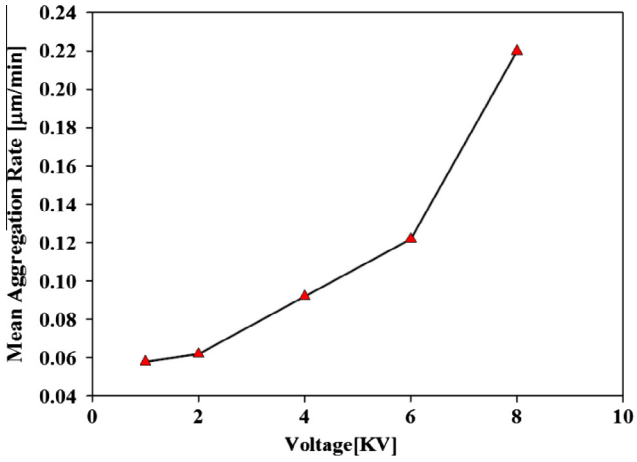

Fig. 5. Average aggregation rate (µm/min) at an asphaltene concentration of 1 g/l for asphaltene Type A subjected to an electrostatic field at varying voltage. Note that for a specific voltage, the aggregation rate declined with the duration that the voltage was applied (see also Fig. 8 below). Here, the average rate is presented for all the applied voltages.

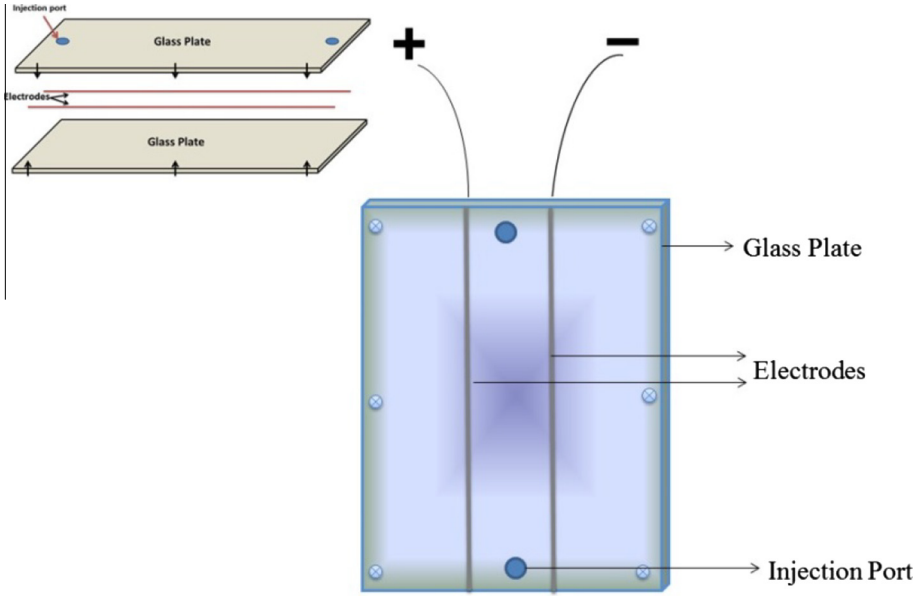

Fig. 3. Schematic representation of the glass micro-model with electrodes inserted.

4. Experimental apparatus

A horizontally oriented glass micro-model, with a pair of opposing electrodes inserted within the model and a microscopic camera, was used to study the asphaltene aggregation rate under electric field. Fig. 2 shows a schematic of the experimental set-up. The electrodes were 6-cm long and the distance between them was 2 cm. The entire electrode length was in contact with the test solution. The model oil (an asphaltene suspension) was injected into the void space between electrodes using a syringe. The injection ports were drilled through the upper glass surface and injection needles were inserted vertically. Schematic representation of the glass micro-model is shown in Fig. 3. The electrodes extended out of the model so that they could be connected to the signal generator. An electric field was generated with a high-voltage, direct current power supply (Sanaye Amouzeshi Co.) capable of supplying voltages up to 13 kV.

Two types of microscopic camera were used: an optical microscope (model E200 Nikon Instrument Inc., USA) and a microscope eyepiece camera (Dino-Eye, AnMo Electronics Corporation, Taiwan) were used to monitor the asphaltene aggregation. To create images with desirable contrast, the glass micro-model was placed on a light panel and at least six images at different locations of the model were taken for each data point to obtain more reliable results. Aggregate size was measured and analyzed with Image J software [43].

5. Experimental procedure

After preparing the model oil according to the aforementioned procedure, the solution was quickly injected into the micro-model by a syringe. The micro-model void space was completely filled with the model oil and then the injection ports were closed and sealed. The electrostatic field applied to the solution while both the asphaltene aggregate size and its aggregation rate were carefully observed for each test using a camera mounted on the microscope. Finally, the average asphaltene aggregate diameter and particle size distribution were measured as a function of time using image-processing software at pre-defined time intervals.

6. Results and discussion

Fig. 4 shows the effect of the high voltage direct current on the average (mean) aggregate size of the Type A asphaltene particles. Similar results were obtained for the other two asphaltene types and only one type is presented here for the sake of brevity. Each experimental data point in Fig. 4 shows the average diameter of asphaltene aggregates observed at a specific time intervals for an 80-min duration; the average diameter is noted to increase with voltage. This behavior can be explained by the fact that the asphaltene particles respond to the electrostatic field by polarizing and folding toward each other. As higher voltage is applied, more polarization and aggregation occur. Based on the results shown in Fig. 4,

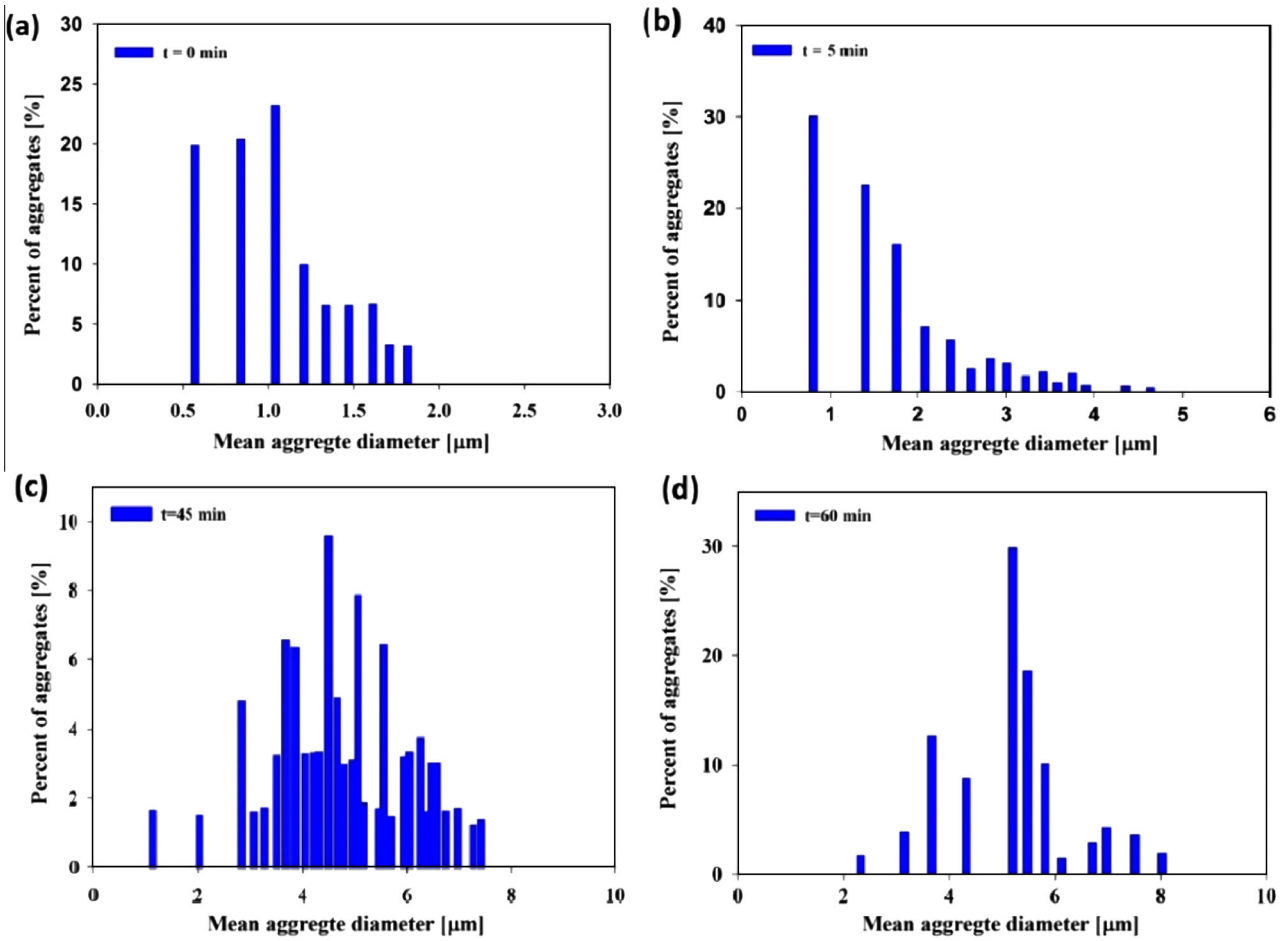

Fig. 6. Aggregate size distribution for asphaltene Type A under applied 1 kV electric potential (a) at initial time step-first seconds of exposure; (b) after 5 min; (c) after 45 min, and; (d) after 60 min.

the average (mean) aggregation rate for the asphaltene Type A was calculated and is illustrated in Fig. 5 for the applied voltages. The average values presented in Fig. 5 are the mean values for each data set of Fig. 4 for the test duration and intended to show the effect of voltage on aggregation rate in a holistic view. It can be observed that the aggregation rate of asphaltene particles increases with the intensity of the electrostatic field. This behavior shows a direct effect of the electrostatic field on asphaltene aggregation; only the electro-static field strength varies while the precipitant concentration remains constant. Thus, the higher asphaltene particle aggregation cannot be a result of the added precipitant.

Fig. 6 demonstrates an increase in aggregate size of the Type A asphaltene particles under a 1 kV potential. Note that the size scale (horizontal axis) is increased so that the distribution can be clearly observed for all time intervals. The initial size distribution is shown in Fig. 6(a), where the majority of particles are smaller than 1.2 microns and no particles are larger than 2 microns. When a 1 kV potential is applied, the average aggregate size of asphaltene particles are observed (Fig. 6b and c) to increase with time so that the majority of particles were larger than 5 microns after 1 h. It is worth noting that the minimum detectable particle size was 0.5 μm and the asphaltene particles were assumed to be spherical.

In Fig. 7 below, optical images of the asphaltene aggregation process at different times and under potential of 6 kV are shown. All images have the same scale and clearly show a trend of aggregation, increasing in size.

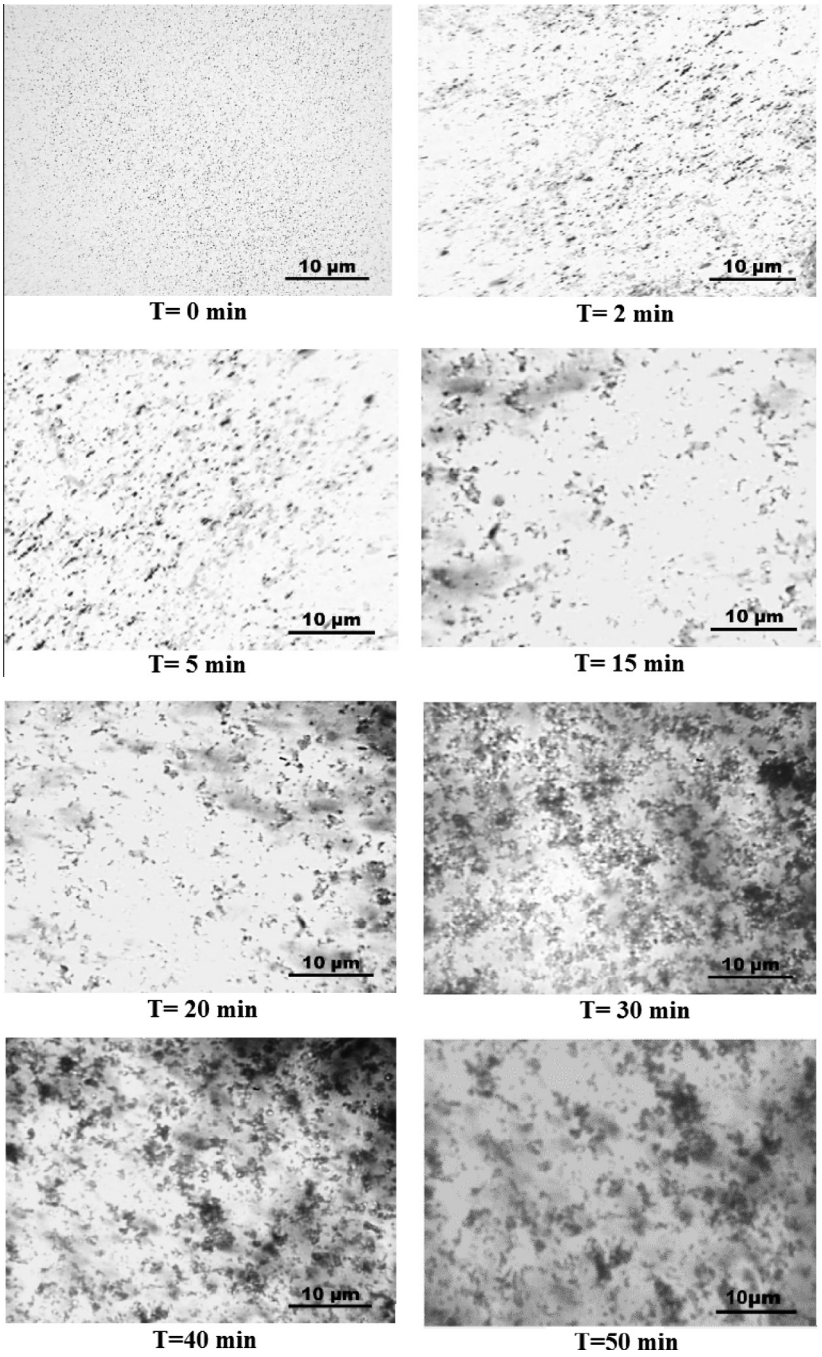

Fig. 7. Optical images of the model oil consisting of 1 g/l solution of asphaltene Type A under 6 kV potential.

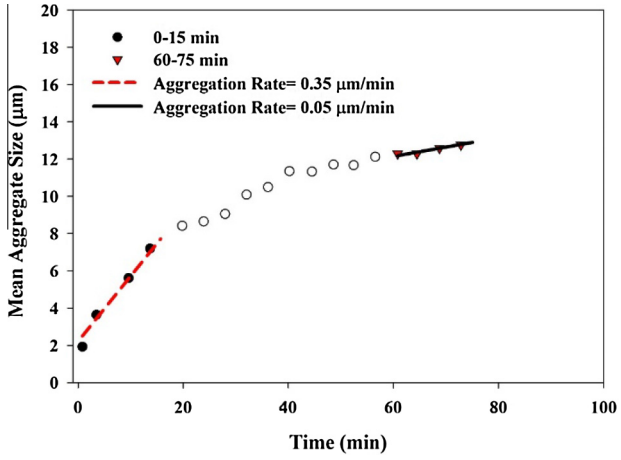

Fig. 8. Aggregation rate as a function of time for asphaltene Type A, under potential of 6 kV. The initial rate is approximately 0.35 µm/min, while the rate after 60 min decreased to approx. 0.05 µm/min.

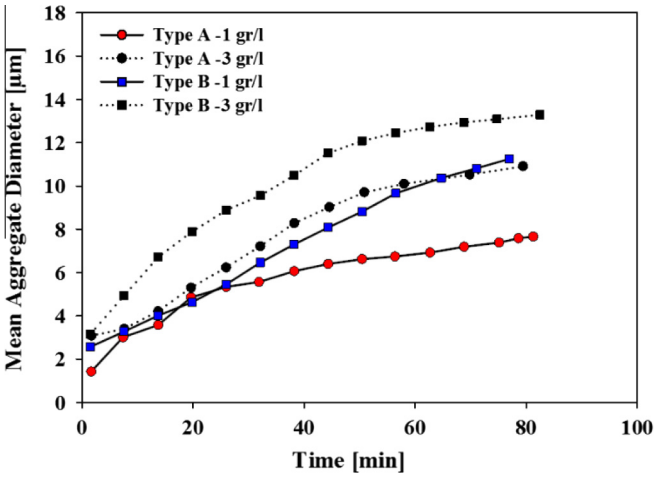

Fig. 9. The effect of asphaltene concentration on average aggregate size for asphaltene Types A and B. The average aggregate size of asphaltene Types A and B, are larger when the concentration is higher, as shown here for two concentrations that were both subjected to a 2 kV electrical potential.

Table 3
Properties of three asphaltenes studied in this work.

Asphaltene	N + O + S (wt.%)	Hydrogen content (wt.%)	Complexity
Type A	12.45	7.19	Medium
Type B	18.68	6.74	Highest
Type C	12.43	7.71	Lowest

Fig. 8 compares the asphaltene aggregation rate under a constant electrostatic voltage of 6 kV. As shown in the figure, the asphaltene aggregates grow at a rate about seven times faster at the initial time intervals than the ultimate time intervals. After some time, the growth rate declined. This behavior could be explained by the fact that an unstable fraction of asphaltene particles is more polar with a higher di-electric constant and metal content that responds quickly to the electric field [44,45]. Therefore, exposure to an electric potential will result in faster precipitation of the unstable fraction compared to the rest of the asphaltene particles and hence a decreasing aggregation rate will be observed.

Fig. 9 elucidates the effect of asphaltene concentration on the average asphaltene aggregate size under a constant 2 kV electrostatic field for two asphaltene particles, Type A and B. As shown in this figure, the asphaltene aggregate size increased for both types when the concentration of asphaltene particles in the mixtures is increased. In addition, faster aggregation for the asphaltene particles was observed for higher asphaltene concentrations.

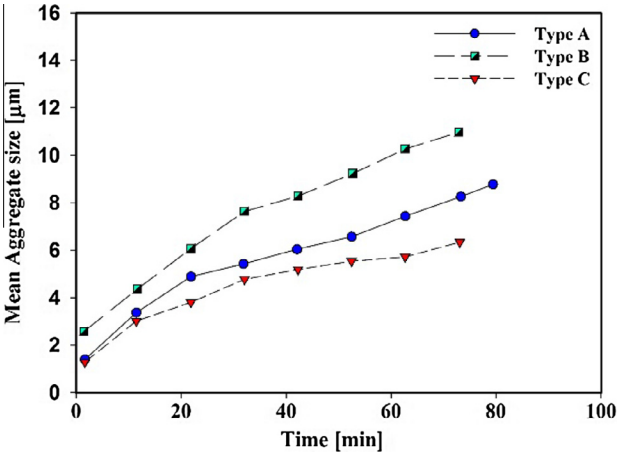

Fig. 10. The average aggregate size for asphaltene particles with asphaltene concentration of 1 g/l subjected to a 2 kV electrostatic field.

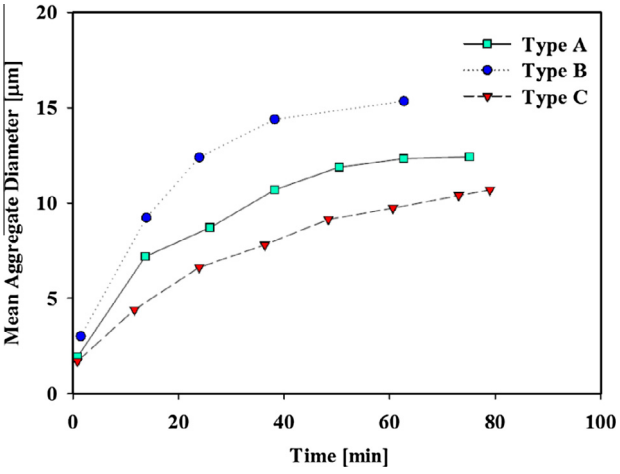

Fig. 11. The average aggregate diameter of asphaltene particles in model oil with asphaltene concentration of 1 g/l subjected to a 6 kV electrostatic field.

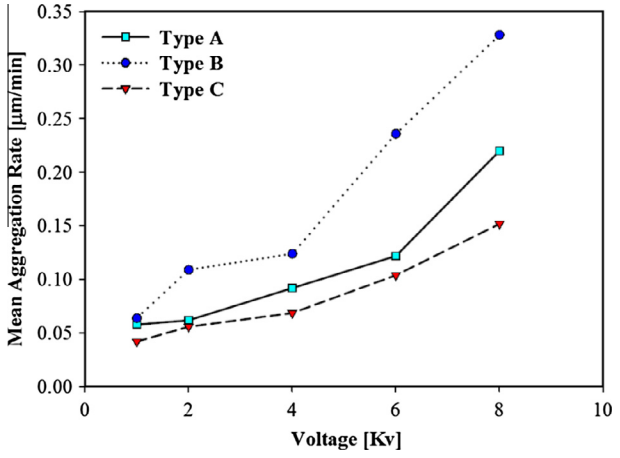

Fig. 12. The effect of voltage on aggregation rate of three asphaltene types.

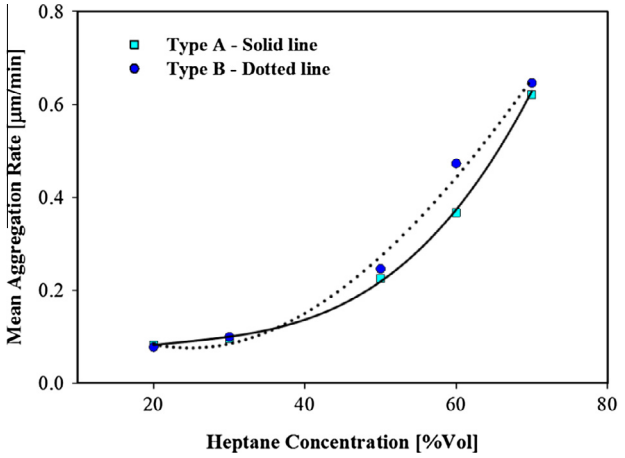

Fig. 13. Effect of precipitant concentration on the mean aggregation rate of asphaltene particles. Increasing the n-heptane concentration has the effect of increasing the average aggregation rate of asphaltene Type A (solid line) and Type B (dotted line) when subjected to a 4 kV electrostatic field. Note that the effect is similar for both asphaltene types.

Increasing the asphaltene concentration of the model oil would increase the solution viscosity to a limited extent. It was shown by Maqbool et al. that increasing the asphaltene solution viscosity decreases particle collision frequency and hence their aggregation rate [39]. However, in the case of electrostatic field, due to the larger number of asphaltene particles at the higher concentrations, particle collisions and aggregation chances are enhanced.

The analysis of asphaltene samples and proposed structure is described in a previous section. Table 3 shows a comparison between some structural properties of the asphaltene samples such as total hetero-atom content, hydrogen content, and structural complexity. Hetero-atom content of asphaltene directly controls its polarity [46]. Thus, it is expected that Type B asphaltene, with highest hetero-atom content and a larger number of aromatic cycles, be more prone to ionization when exposed to an electric field compared with the other two asphaltene types. This ionization will enhance the asphaltene particles' surface charge properties [11] and will result in a higher aggregation rate. Our results show this to be true: asphaltene Type B, with highest hetero-atom content, has the highest aggregation rate when exposed to electrical potential.

The effect of molecular structure on the average aggregate diameter of asphaltene particles under electrostatic field at two voltages was considered using the results presented in Figs. 10 and 11. As can be observed, the Type B asphaltene has a higher aggregation tendency compared to those particles of Type A and C. Also, the same observation can be made for the aggregation rate of the Type B asphaltene particles. Fig. 12 shows that the highest aggregation rate is observed for the Type B asphaltene compared to those Type A and C. Since Type B has the highest value of total heteroatom content (elucidated by the structural analysis, as mentioned earlier), this fact could be a plausible explanation for this behavior. In addition, comparison of the same results shown in Figs. 10–12 indicates that the higher voltage can cause more asphaltene aggregation at a higher aggregation rate for all three samples.

The effect of n-heptane concentration on the average aggregation rate can be seen on Fig. 13. The higher ratio of n-heptane resulted in a higher aggregation rate for all three types of asphaltene particles (two of them are shown here). It is expected that a mixture with higher n-heptane concentration can precipitate more asphaltene particles which, in turn, results in a higher asphaltene aggregation rate. Note that there is little difference in the aggregation rate between the two types asphaltene types, A and B, and it can be concluded that the sensitivity of asphaltene type B to n-heptane concentration is not significantly greater than other asphaltene types, while it is more sensitive to electric field intensity as was observed in Fig. 12.

7. Conclusions

The effect of electrostatic field on the aggregation rate and aggregate size of asphaltene particles from three different crude oil samples in the mixture of toluene and n-heptane has been investigated. A glass micro-model equipped with two electrodes, an optical microscope and a high voltage direct current power supply were used. In this study, the effect of several parameters—structural properties, electric field strength, asphaltene and precipitant concentration—on the average aggregation size and rate of asphaltene particles were evaluated. Elemental analyses for the three asphaltene samples were carried out and the mass ratios for C, H, N, S and O atoms present in the asphaltene samples were specified. The functional groups on asphaltene molecules were analyzed using the FTIR technique. It was found that asphaltene molecules with larger chromophore and higher complexity exhibits faster aggregation behavior while exposed to the electric field. In addition, asphaltene aggregation rate is directly proportional to the number of hetero-atoms on asphaltene molecules.

Results show that the higher aggregation rate of asphaltene particles was observed when the electric field with higher voltage was applied to the mixture. In addition, a descending trend of aggregation rate was observed during each test, which indicates faster precipitation of the unstable fraction of asphaltene particles (more polar particles with higher metal content and di-electric constant) relative to the rest of the asphaltene particles. The asphaltene aggregate size increased with increasing the concentration of asphaltene particles in the mixtures, which is the result of increased collisions between particles. Also, faster aggregation was observed at higher n-heptane (precipitant) concentrations subjected to a electric field.

In conclusion, an electrostatic field could highly affect the aggregate size and aggregation rate of asphaltene particles. In fact, under the electrostatic field, the asphaltene particles tend to get aggregated faster and this, in turn, may result in faster asphaltene deposition. The results show that the asphaltene electro-kinetic behavior is mainly controlled by structural characteristics such as hetero-atom content, structural complexity and molecular characteristics.

References

[1] Andersen SI, Speight JG. Thermodynamic models for asphaltene solubility and precipitation. J Petrol Sci Eng 1999;22(1):53–66.
[2] Artok L, Su Y, Hirose Y, Hosokawa M, Murata S, Nomura M. Structure and reactivity of petroleum-derived asphaltene. Energy Fuels 1999;13(2):287–96.
[3] Borton D, Pinkston DS, Hurt MR, Tan X, Azyat K, Scherer A, et al. Molecular structures of asphaltenes based on the dissociation reactions of their ions in mass spectrometry. Energy Fuels 2010;24(10):5548–59.
[4] Gawrys KL, Matthew Spiecker P, Kilpatrick PK. The role of asphaltene solubility and chemical composition on asphaltene aggregation. Pet Sci Technol 2003;21(3–4):461–89.
[5] Sheu EY. Petroleum asphaltene properties, characterization, and issues. Energy Fuels 2002;16(1):74–82.
[6] Andersen SI, Stenby EI. Thermodynamics of asphaltene precipitation and dissolution investigation of temperature and solvent effects. Fuel Sci Technol Int 1996;14(1–2):261–87.
[7] Leontaritis K, Mansoori G. Asphaltene flocculation during oil production and processing: A thermodynamic colloidal model. Paper SPE; 1987, 16258, 4–6.
[8] Xie K, Karan K. Kinetics and thermodynamics of asphaltene adsorption on metal surfaces: a preliminary study. Energy Fuels 2005;19(4):1252–60.
[9] Joshi NB, Mullins OC, Jamaluddin A, Creek J, McFadden J. Asphaltene precipitation from live crude oil. Energy Fuels 2001;15(4):979–86.
[10] Victorov AI, Firoozabadi A. Thermodynamic micellizatin model of asphaltene precipitation from petroleum fluids. AIChE J 1996;42(6):1753–64.

[11] Khvostichenko DS, Andersen SI. Electrodeposition of asphaltenes. 1. Preliminary studies on electrodeposition from oil−heptane mixtures. Energy Fuels 2009;23(2):811–9.
[12] Khvostichenko DS, Andersen SI. Electrodeposition of asphaltenes. 2. Effect of resins and additives†. Energy Fuels 2010;24(4):2327–36.
[13] Taylor SE. The electrodeposition of asphaltenes and implications for asphaltene structure and stability in crude and residual oils. Fuel 1998;77(8):821–8.
[14] Precksho G, DeLisle N, Cottrell C, Katz D. Asphaltic substances in crude oils. Trans. AIME 1943;151(01):188–205.
[15] Ali Mansoori G. Modeling of asphaltene and other heavy organic depositions. J Petrol Sci Eng 1997;17(1):101–11.
[16] Lichaa PM, Herrera L. In: Electrical and other effects related to the formation and prevention of asphaltene deposition problem in Venezuelan crudes, SPE oilfield chemistry symposium. Society of Petroleum Engineers; 1975.
[17] Goual L, Horváth-Szabó G, Masliyah JH, Xu Z. Characterization of the charge carriers in bitumen. Energy Fuels 2006;20(5):2099–108.
[18] Eldib L. In: The solvation, ionic and electrophoretic properties of colloidal asphaltenes in petroleum. Preprints of ACS Symp., Washington, DC; 1962. 1962. p. 31–42.
[19] Moore E, Crowe C, Hendrickson A. Formation effect and prevention of asphaltene sludges during stimulation treatments. J Petrol Technol 1965;17(09):1023–8.
[20] Wright JR, Minesinger RR. The electrophoretic mobility of asphaltenes in nitromethane. J Colloid Sci 1963;18(3):223–36.
[21] Leon O, Rogel E, Espidel J, Torres G. Asphaltenes: structural characterization, self-association, and stability behavior. Energy Fuels 2000;14(1):6–10.
[22] González G, Neves GB, Saraiva SM, Lucas EF, dos Anjos de Sousa M. Electrokinetic characterization of asphaltenes and the asphaltenes-resins interaction. Energy Fuels 2003;17(4):879–86.
[23] Idem RO, Ibrahim HH. Kinetics of CO_2-induced asphaltene precipitation from various Saskatchewan crude oils during CO_2 miscible flooding. J Petrol Sci Eng 2002;35(3):233–46.
[24] Al-Huraibi N, Belhaj HA. In: Modeling of crude oil asphaltenes deposition: In-depth colloidal prospective. SPE production and operations conference and exhibition. Society of Petroleum Engineers; 2010.
[25] Eow JS, Ghadiri M. Electrostatic enhancement of coalescence of water droplets in oil: a review of the technology. Chem Eng J 2002;85(2):357–68.
[26] Leontaritis K. In: Asphaltene deposition: a comprehensive description of problem manifestations and modeling approaches, SPE production operations symposium. Society of Petroleum Engineers; 1989.
[27] Alkafeef SF. In: An investigation of the stability of colloidal asphaltene in petroleum reservoirs. SPE international symposium on oilfield chemistry. Society of Petroleum Engineers; 2001.
[28] Fotland P, Anfindsen H. Electrical conductivity of asphaltenes in organic solvents. Fuel Sci Technol Int 1996;14(1–2):101–15.
[29] Behar E, Hasnaoui N, Achard C, Rogalski M. Study of asphaltene solutions by electrical conductivity measurements. Oil Gas Sci Technol 1998;53(1):41–50.
[30] Evdokimov IN, Losev AP. Electrical conductivity and dielectric properties of solid asphaltenes. Energy Fuels 2010;24(7):3959–69.
[31] Kokal S, Tang T, Schramm L, Sayegh S. Electrokinetic and adsorption properties of asphaltenes. Colloids Surf A 1995;94(2):253–65.
[32] Leon O, Rogel E, Torres G, Lucas A. Electrophoretic mobility and stabilization of asphaltenes in low conductivity media. Pet Sci Technol 2000;18(7–8):913–27.
[33] Parra-Barraza H, Hernández-Montiel D, Lizardi J, Hernández J, Herrera Urbina R, Valdez MA. The zeta potential and surface properties of asphaltenes obtained with different crude oil/n-heptane proportions. Fuel 2003;82(8):869–74.
[34] Szymula M, Janusz W, Jabloriski J. Electrochemical properties of asphaltene particles in aqueous solutions. J Dispersion Sci Technol 2000;21(6):785–802.
[35] Yen TF, Chilingarian GV. Structural parameters from asphaltenes and their geochemical significance. Dev Petrol Sci 1994;40:159–78.
[36] Hashmi SM, Firoozabadi A. Controlling nonpolar colloidal asphaltene aggregation by electrostatic repulsion. Energy Fuels 2012;26(7):4438–44.
[37] Mohamed RS, Ramos AC, Loh W. Aggregation behavior of two asphaltenic fractions in aromatic solvents. Energy Fuels 1999;13(2):323–7.
[38] Alboudwarej H, Jakher RK, Svrcek WY, Yarranton HW. Spectrophotometric measurement of asphaltene concentration. Pet Sci Technol 2004;22(5–6):647–64.
[39] Maqbool T, Balgoa AT, Fogler HS. Revisiting asphaltene precipitation from crude oils: a case of neglected kinetic effects. Energy & Fuels 2009;23:3681–6.
[40] Amin JS, Nikooee E, Ghatee M, Ayatollahi S, Alamdari A, Sedghamiz T. Investigating the effect of different asphaltene structures on surface topography and wettability alteration. Appl Surf Sci 2011;257(20):8341–9.
[41] Semple KM, Cyr N, Fedorak PM, Westlake DW. Characterization of asphaltenes from Cold Lake heavy oil: variations in chemical structure and composition with molecular size. Can J Chem 1990;68(7):1092–9.
[42] Calemma V, Iwanski P, Nali M, Scotti R, Montanari L. Structural characterization of asphaltenes of different origins. Energy Fuels 1995;9(2):225–30.
[43] Schneider CA, Rasband WS, Eliceiri KW, Schindelin J, Arganda-Carreras I, Frise E, et al. NIH image to imageJ: 25 years of image analysis. Nat Methods 2012;9(7):671–5.
[44] Wattana P, Fogler HS, Yen A, Carmen Garcìa MD, Carbognani L. Characterization of polarity-based asphaltene subfractions. Energy Fuels 2005;19(1):101–10.
[45] Maqbool T, Balgoa AT, Fogler HS. Revisiting asphaltene precipitation from crude oils: a case of neglected kinetic effects. Energy Fuels 2009;23(7):3681–6.
[46] Boduszynski MM. Asphaltenes in petroleum asphalts: composition and formation. Am Chem Soc Div Pet Chem Prepr; (United States) 1979, 24, (CONF-790917-(vol. 24)(No. 4)).